

Inhibitory Effect of Citrus Nobiletin on Phorbol Ester-induced Skin Inflammation, Oxidative Stress, and Tumor Promotion in Mice¹

Akira Murakami, Yoshimasa Nakamura, Koji Torikai, Takuji Tanaka, Teruaki Koshiba, Koichi Koshimizu, Shigeru Kuwahara, Yasuo Takahashi, Kazunori Ogawa, Masamichi Yano, Harukuni Tokuda, Hoyoku Nishino, Yoshihiro Mimaki, Yutaka Sashida, Susumu Kitanaka, and Hajime Ohigashi²

Department of Biotechnological Science, Faculty of Biology-Oriented Science and Technology, Kinki University, Wakayama 649-6493 [A. M., T. K., K. K.]; Division of Applied Life Sciences, Graduate School of Agriculture, Kyoto University, Kyoto 606-8502 [Y. N., K. T., H. O.]; First Department of Pathology, Kanazawa Medical University, Ishikawa 920-0293 [T. T.]; Research and Development Division, Wakayama Agricultural Processing Research Corporation, Nagagun, Wakayama 649-6112 [S. K., Y. T.]; Department of Citriculture, Fruit Tree Research Station, Shizuoka 424-0292 [K. O., M. Y.]; Department of Biochemistry, Kyoto Prefecture University of Medicine, Kyoto 602-0841 [H. T., H. N.]; Laboratory of Medicinal Plant Science, School of Pharmacy, Tokyo University of Pharmacy and Life Science, Tokyo 192-0392 [Y. M., Y. S.]; and Laboratory of Pharmacognosy, College of Pharmacy, Nihon University Chiba 274–8555 [S. K.], Japan

ABSTRACT

The intake of citrus fruits has been suggested as a way to prevent the development of some types of human cancer. Nitric oxide (NO) is closely associated with the processes of epithelial carcinogenesis. We attempted a search for NO generation inhibitors in *Citrus unshiu*. The active constituent was traced by an activity-guiding separation. NO and superoxide (O_2^-) generation was induced by a combination of lipopolysaccharide and IFN- γ in mouse macrophage RAW 264.7 cells, and by 12-*O*-tetradecanoylphorbol-13-acetate (TPA) in differentiated human promyelocyte HL-60, respectively. Expression of inducible NO synthase and cyclooxygenase 2 proteins were detected by Western blotting. The *in vivo* anti-inflammatory and antitumor promoting activities were evaluated by topical TPA application to ICR mouse skin with measurement of edema formation, epidermal thickness, leukocyte infiltration, hydrogen peroxide production, and the rate of proliferating cell nuclear antigen-stained cells. As a result, nobiletin, a polymethoxyflavonoid, was identified as an inhibitor of both NO and O_2^- generation. Nobiletin significantly inhibited two distinct stages of skin inflammation induced by double TPA application [first stage priming (leukocyte infiltration) and second stage activation (oxidative insult by leukocytes)] by decreasing the inflammatory parameters. It also suppressed the expression of cyclooxygenase-2 and inducible NO synthase proteins and prostaglandin E_2 release. Nobiletin inhibited dimethylbenz[*a*]anthracene (0.19 μ mol)/TPA (1.6 nmol)-induced skin tumor formation at doses of 160 and 320 nmol by reducing the number of tumors per mouse by 61.2% ($P < 0.001$) and 75.7% ($P < 0.001$), respectively. The present study suggests that nobiletin is a functionally novel and possible chemopreventive agent in inflammation-associated tumorigenesis.

INTRODUCTION

The intake of citrus fruits has been found to be beneficial for cancer prevention by epidemiological survey (1). Citrus fruit contains several classes of chemopreventive agents, *e.g.*, limonoids and their glycosides (2, 3), *d*-limonene (4, 5), several flavonoids (6) such as hesperidin (7, 8), and glyceroglycolipids (9). Our group has demonstrated that auroptene, which is a coumarin-related compound widely occurring in citrus juices (*e.g.*, grapefruit), exhibited a marked inhibition of

TPA³-induced O_2^- and hydroperoxide production and inhibited skin tumor promotion in mice by topical application (10). Oral administration of auroptene also inhibited 4-nitroquinoline-1-oxide-induced oral carcinogenesis in rats (11) and azoxymethane-induced aberrant crypt (12) and adenocarcinoma formation (13) in the rat colon.

Nitric oxide (NO), a gaseous free radical, is released by a family of enzymes, constitutive NO synthase and an inducible one (iNOS; Ref. 14) with the formation of stoichiometric amounts of L-citrulline from L-arginine (15). iNOS-mediated excessive and prolonged NO generation has attracted attention because of its relevance to epithelial carcinogenesis (16–18). NO has been reported to cause mutagenesis (19) and deamination of DNA bases (20) and to form carcinogenic *N*-nitrosoamines (21). With respect to the role of NO in the postinitiation phase, it should be noted that it plays important roles in such inflammatory responses as edema formation and hyperplasia, as well as in papilloma development in mouse skin (22, 23). NO is also involved in the production of VEGF (24), the overexpression of which induces angiogenesis, vascular hyperpermeability, and accelerated tumor development (25). Topical application of TPA to mice led to edema and papilloma formation by enhancing COX-2 protein expression. Specific COX-2 inhibitors (26, 27) could counteract these biological events. Collectively, suppression of enzyme induction and the activities of iNOS/COX-2 is a new paradigm for the prevention of carcinogenesis in several organs, including the stomach and colon. In fact, some dietary compounds, including chemopreventive agents (28–31) and the extracts from edible plants (32), have recently been reported to suppress iNOS-mediated NO generation.

The present study was undertaken to search for NO generation inhibitors in *Citrus unshiu* (satsuma mandarin), the most popular citrus fruit in Japan, by activity-guiding fractionation and purification, using a combined LPS- and IFN- γ -induced NO generation test in mouse macrophage RAW 264.7 cells. As a result, we identified a polymethoxyflavonoid, nobiletin, to be a dual inhibitor of both NO and O_2^- generation in leukocytes. Wei *et al.* (33) reported that double applications of TPA to mouse skin led to excessive ROS production. Ji and Marnett (34) termed each application as “priming” (the first stage illustrated by leukocyte recruitment, maturation, and infiltration of inflammatory leukocytes such as polymorphonuclear leukocytes and macrophages into inflamed lesions) and “activation” (the second stage illustrated by ROS production from accumulated leukocytes). Our research addressed whether nobiletin inhibits the priming and/or activation stages in this double application model. In addition, the

Received 1/18/00; accepted 7/13/00.

The costs of publication of this article were defrayed in part by the payment of page charges. This article must therefore be hereby marked *advertisement* in accordance with 18 U.S.C. Section 1734 solely to indicate this fact.

¹ Supported by the Grant-in-Aid for the Japan Society for the Promotion of Science (to Y. N.); the Program for Promotion of Basic Research Activities for Innovative Biosciences (to A. M., K. O., M. Y., H. T., H. N., K. K., H. O.); the 2nd Term for a Comprehensive 10-year Strategy for Cancer Control from the Ministry of Health and Welfare of Japan, Scientific Research (Nos. 10671782 and 11138255) from the Ministry of Education, Science, Sports and Culture of Japan; and by Grant HS-52260 for a comprehensive research project on health sciences focusing on drug innovation from the Japan Health Sciences Foundation (to T. T.).

² To whom requests for reprints should be addressed, at Division of Applied Life Sciences, Graduate School of Agriculture, Kyoto University, Kyoto 606-8502, Japan. Phone: 81-75-753-6281; Fax: 81-75-753-6284; E-mail: ohigashi@kais.kyoto-u.ac.jp.

³ The abbreviations used are: TPA, 12-*O*-tetradecanoylphorbol-13-acetate; COX, cyclooxygenase; DMBA, 7,12-dimethylbenz[*a*]anthracene; HPLC, high-performance liquid chromatography; IL, interleukin; iNOS, inducible NO synthase; IR, inhibitory rate; LPS, lipopolysaccharide; O_2^- , superoxide; PCNA, proliferating cell nuclear antigen; PG, prostaglandin; ROS, reactive oxygen species; TNF, tumor necrosis factor; VEGF, vascular endothelial growth factor.

inhibitory effect of nobiletin on mouse skin tumor promotion using a two-stage carcinogenesis model was investigated.

MATERIALS AND METHODS

Chemicals, Cells, and Animals. TPA was obtained from Research Biochemicals International (Natick, MA). DMEM and fetal bovine serum were purchased from Gibco RBL (Grand Island, NY). LPS (*Escherichia coli* serotype 0127, B8) was purchased from Difco Labs (Detroit, MI) and IFN- γ from Genzyme (Cambridge, MA). Cytochrome *c* was obtained from Sigma (St. Louis, MO). Luteolin was obtained from Extrasynthèse (Genay, France). All other chemicals were purchased from Wako Pure Chemical Industries, Co., Ltd. (Osaka, Japan). HL-60 cells were purchased from American Type Culture Collection (Manassas, VA). RAW 264.7 cells were kindly donated by Ohtsuka Pharmaceutical Co. Ltd. (Ohtsu, Japan). Female ICR mice, ages 6–7 weeks, were obtained from Japan SLC (Shizuoka, Japan).

Isolation and Identification of Nobiletin. Whole fruit of *C. unshiu* (10-kg fresh weight), harvested in Wakayama Prefecture, Japan, were processed by an FMC in-line citrus juice extractor (FMC Corporation, Chicago, IL) to produce cold-pressed oil (150 ml). Most of the monoterpenes, *d*-limonene being the major constituent (~90%), were removed from the oil by evaporation under reduced pressure at 80°C. Then, the terpene-less oil was separated into useful fractions by monitoring the inhibition of NO generation. The active fraction was separated by silica gel column chromatography (*n*-hexane/ethyl acetate, stepwise method), then by preparative TLC (*n*-hexane/ethyl acetate, 1:1), and finally by HPLC (column: μ Bondasphere C₁₈; Waters, Milford, MA; 19 \times 150 mm; elute: 70% methanol in water; flow rate: 7.0 ml/min; detection: UV_{254 nm}) to produce nobiletin (84 mg; retention time at 16.9 min; purity >98%). The chemical identity was confirmed by comparison of its spectral data with those reported previously (35).

NO Generation Test. Murine macrophage cell line RAW 264.7 cells grown confluent in 2 ml of DMEM on a 60-mm dish were treated with LPS (100 ng/ml), tetrahydrobiopterin (10 mg/ml), IFN- γ (100 units/ml), L-arginine (2 mM), and a test compound (0, 25, 50, or 100 μ M). After 18 h, the levels of NO₂⁻ were measured by Griess assay. Cytotoxicity was measured by a 3-(4,5-dimethylthiazol-2-yl)-2,5-diphenyltetrazolium bromide (MTT) assay. Each experiment was done independently in duplicate twice, and the data are expressed as mean \pm standard deviation (SD) values.

Western Blotting. Confluent RAW 264.7 cells were stimulated and incubated in the same manner as described above. After the cells were washed, a boiling lysis solution was added to the cells, which were then scraped from the dish, sonicated, and boiled for 10 min. Protein concentrations were determined using a DC Protein Assay kit (Bio-Rad Laboratories, Hercules, CA), and BSA was used as the standard. Ten- μ g proteins were separated on 10% polyacrylamide gels and electrophoretically transferred onto polyvinylidene difluoride membranes (Millipore, MA). After blocking, the membranes were incubated with a primary antibody (antimouse iNOS, 1:1000 dilution; Affinity Bio-reagents, Inc., Golden, CO), and then with a secondary antibody (peroxidase-conjugated swine antirabbit IgG, 1:1000 dilution; Dako, Glostrup, Denmark). The blots were developed using an ECL detection kit (Amersham Life Science, Buckinghamshire, United Kingdom). The antibodies were stripped and the blots were successively reprobated with each primary antibody. The first incubation was with: (a) goat antirat COX-2 antibody [cross-reacts with mouse counterparts, 1:1000 dilution (Santa Cruz Biotechnology, Inc., Santa Cruz, CA)]; or (b) rabbit polyclonal anti- β -actin antibody (1:1000 dilution; Biochemical Technologies, Stoughton, MA). Each membrane was then incubated with a corresponding secondary antibody: (a) peroxidase-conjugated rabbit anti-goat IgG (1:1000 dilution; Dako); and (b) peroxidase-conjugated swine antirabbit IgG (1:1000 dilution; Dako). The levels of iNOS or COX-2 bands were corrected using those of β -actin as an internal standard. Each experiment was done independently in duplicate twice, and the data are expressed as mean \pm SD values.

Double TPA Treatment of Mouse Skin. The double TPA treatment experiment was performed as reported previously (36). Briefly, the back of each mouse was shaved using surgical clippers 2 days before each experiment; each experimental group consisted of five mice. Nobiletin (810 nmol in 100 μ l of acetone) was applied topically to the shaved area of the dorsal skin 30 min before application of a TPA solution (8.1 nmol in 100 μ l of acetone). In the

double-treatment protocol, the same doses of TPA and the test compounds or acetone were applied twice at an interval of 24 h. We divided the mice into five groups as follows: group 1 (acetone \times 2/acetone \times 2); group 2 (acetone-TPA/acetone-TPA); group 3 (nobiletin-TPA/nobiletin-TPA); group 4 [nobiletin (priming)-TPA/acetone-TPA]; and group 5 [acetone-TPA/nobiletin (activation)-TPA].

Measurement of H₂O₂ and Edema Formation in Mouse Skin. Measurement of the levels of H₂O₂ and edema formation was done as reported previously (36). In brief, mice treated by the double-treatment protocol were sacrificed 1 h after the second TPA treatment. Skin punches (epidermis and dermis) were obtained with an 8-mm-diameter cork borer and were weighed with an analytical balance. The skin punches were minced in 3 ml of 50 mM phosphate buffer (pH 7.4) containing 5 mM sodium azide and then homogenized at 4°C for 30 s twice. The homogenate was centrifuged at 10,000 \times g for 20 min at 4°C. The H₂O₂ content was determined by the phenol red-horse-radish peroxidase method.

Histological Examination. Histological examinations were done as reported previously (36). Briefly, excised skin was fixed in 10% buffered formalin and then embedded in paraffin. For each skin section (3 μ m) stained with H&E, the thickness of the epidermis from the basal layer to the stratum corneum was measured at five equidistant interfollicular sites using a Leica Q500IW-EX image analysis system (Leica, Co. Ltd., Tokyo, Japan) with a Leica DMRE HC microscope (Leica, Co. Ltd.). The number of infiltrating leukocytes was counted at five different areas.

PCNA Immunohistochemistry. A PCNA immunohistochemistry was done as reported previously (36). Briefly, skin sections were treated with 1.2% H₂O₂ in absolute methanol for 30 min and were stained by the indirect avidin-biotin-horseradish peroxidase method (ABC standard; Vector laboratories, Burlingame, CA). Color development with diaminobenzidine (Vector laboratories) was monitored by the appearance of normal PCNA brown staining in the normal epidermis. The primary antibody to PCNA (PC10; Boehringer Mannheim, Mannheim, Germany) was applied at a 1:300 concentration overnight at 4°C. The PCNA index was counted at six different areas of each section using the image analysis system and was expressed as the number of positive squamous cells divided by the total number of squamous cells \times 100.

O₂⁻ Generation in Differentiated HL-60 Cells. An inhibitory test of TPA-induced O₂⁻ generation was performed as reported previously (36). Briefly, differentiated HL-60 cells were treated with 100 nM TPA, appropriate concentrations of the test compounds, and 1 mg/ml cytochrome *c*. After incubation at 37°C for 30 min, the level of extracellular O₂⁻ was measured by cytochrome *c* reduction. Each experiment was done in duplicate independently twice, and the data are expressed as mean \pm SD values.

Cellular Uptake. Differentiated HL-60 cells were incubated and treated in the same manner as described above. For extracellular measurement, after the cell suspension was centrifuged, supernatant was collected, and the cells were washed with media three times to combine the media used for washing with the supernatant. The combined solution (4 ml) was partitioned between distilled water (1 ml) and ethyl acetate (5 ml). For intracellular measurement, cells were suspended in iced water and ethyl acetate (5 ml each) and were sonicated for 10 s twice on ice. The ethyl acetate fractions from the intracellular and extracellular samples were separately concentrated *in vacuo* and subjected to HPLC analysis [column: YMC-Pack ODS H-80 J'sphere (4.6 \times 150 mm; Yamamuta Chemical Co. Ltd., Kyoto, Japan); detection: UV_{280 nm} at 45°C with a flow rate of 1.0 ml/min]. Nobiletin and luteolin were detected using 40% acetonitrile in water as an elute at 8.1 min and 25% acetonitrile in water at 3.9 min, respectively. Their incorporation efficiencies were determined by the intracellular:extracellular ratio. Each experiment was done in duplicate independently twice, and the data are expressed as mean \pm SD values.

PGE₂ Determination. RAW 264.7 cells, grown confluent in 2 ml of DMEM on a 60-mm dish, were treated with LPS (100 ng/ml), tetrahydrobiopterin (10 mg/ml), IFN- γ (100 units/ml), L-arginine (2 mM), and a test compound (0, 25, 50, or 100 μ M) dissolved in DMSO (0.5%, v/v). After 18 h, the concentrations of PGE₂ in the media were measured using a commercial experimental kit (Cayman, Ann Arbor, MI), and protein concentrations were determined using a DC Protein Assay kit (Bio-Rad Laboratories). BSA was used as the standard. Each experiment was done in duplicate independently twice, and the data are expressed as mean \pm SD values.

Two-Stage Carcinogenesis Experiment in Mouse Skin. The antitumor promoting activity of nobiletin was examined by a standard initiation-promo-

tion protocol with DMBA and TPA, as reported previously (10). One group was composed of 15–17 female ICR mice. These mice were given commercial rodent pellets and fresh tap water *ad libitum*, both of which were freshly exchanged twice a week. The back of each mouse was shaved with a surgical clipper 2 days before initiation. Mice at 6 weeks old were initiated with DMBA (0.19 μmol in 100 μl of acetone). One week after initiation, the mice were promoted with TPA (1.6 nmol in 100 μl of acetone) twice a week for 20 weeks. In the other four groups, the mice were treated with nobiletin (40, 80, 160, or 320 nmol in 100 μl of acetone) 40 min before each TPA treatment. The antitumor-promoting activity was evaluated by both the ratio of tumor-bearing mice and the number of tumors that measured more than 1 mm in diameter, per mouse. The data were statistically analyzed using Welch's *t* test for the average number of tumors per mouse and by the χ^2 test for the rates of tumor-bearing mice.

Statistical Analysis. The statistical significance of differences between groups in each assay was assessed by Welch's *t* test, Student's *t* test, or χ^2 test.

RESULTS

Isolation and Identification of Nobiletin. Whole fruit of satsuma mandarins was processed by an FMC in-line citrus juice extractor, which is widely used in fruit juice factories, to produce cold-pressed oil. *d*-Limonene was removed from the oil to be further separated into novel active compounds. The terpene-less oil thus obtained was then separated into useful fractions by monitoring the inhibitory activities toward NO generation. The active fraction was chromatographed on silica gel and finally purified by HPLC to give nobiletin (Fig. 1), the chemical identity of which was elucidated by comparison of the spectral data with those reported previously (35).

Inhibition of NO Generation. Stimulation of RAW 264.7 cells with LPS/IFN- γ for 18 h resulted in NO generation and then nitrite (NO_2^-) accumulation in the media ($40.3 \pm 7.3 \mu\text{M}$). Nobiletin, at a concentration range of 25–100 μM , concentration-dependently suppressed NO_2^- production by 18.6–58.1% (Fig. 2). The inhibitory effect of a red wine polyphenol, resveratrol (37–39), was also examined for comparison of activity, and its inhibitory potency was found to be similar to that of nobiletin. iNOS protein expression was then detected using Western blotting. As also shown in Fig. 2, although being hardly detectable in the cellular lysate without stimulation, iNOS protein was remarkably up-regulated 25-fold 18 h after stimulation. Whereas nobiletin showed a dose-dependent suppression at a concentration range of 25–100 μM (IRs, 32.7–82.0%), resveratrol showed marked inhibition only at a concentration of 100 μM , and activity drastically declined at the concentrations of 50 and 25 μM . Notable cytotoxicity was not observed in any of the experiments (data not shown).

Anti-inflammatory and Antioxidative Activities in Mouse Skin. We then examined whether nobiletin inhibits the priming and/or activation stages using the double-TPA-application model. As shown in Table 1, double TPA applications, at a dose of 8.1 nmol each with a 24-h interval, led to notable edema formation ($42.3 \pm 2.6 \text{ mg/punch}$ in group 2) as compared with the control ($24.7 \pm 4.5 \text{ mg/punch}$ in group 1; $P < 0.001$ versus group 2). Double pretreatment with nobiletin (group 3) 30 min prior to each TPA application suppressed

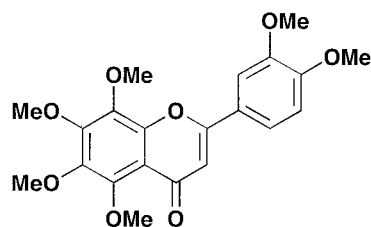


Fig. 1. Chemical structure of nobiletin.

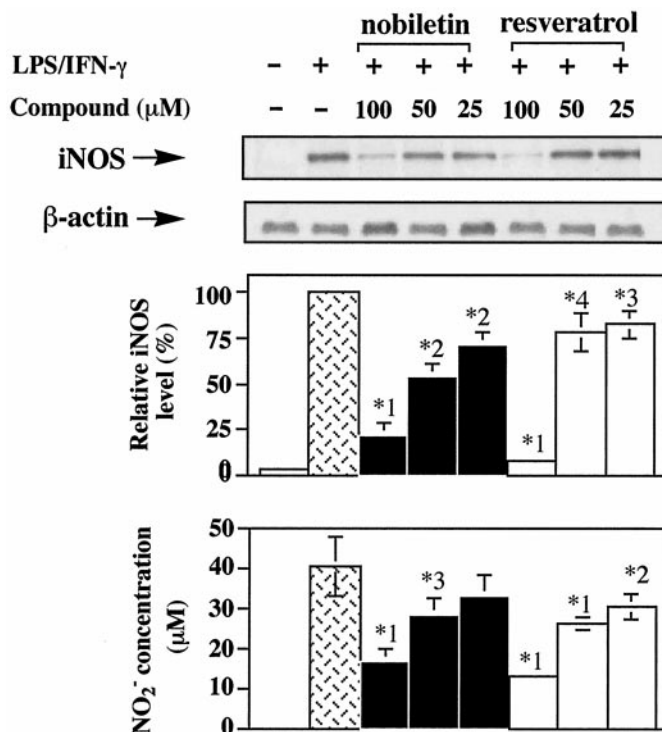


Fig. 2. Inhibitory effects of nobiletin and resveratrol on LPS/IFN- γ -induced NO generation in RAW 264.7 cells. RAW 264.7 cells were treated with LPS (100 ng/ml), BH_4 (10 mg/ml), IFN- γ (100 units/ml), L-arginine (2 mM), and test compound dissolved in DMSO at the indicated concentrations. After 18 h, the levels of NO_2^- were measured by Griess assay. Western blotting was performed as described in "Materials and Methods." The iNOS band levels were corrected by those of β -actin as the internal standard. *1, $P < 0.001$; *2, $P < 0.01$; *3, $P < 0.02$; *4, $P < 0.05$ versus positive control (LPS/IFN- γ) in the Student *t* test. Each experiment was done independently in duplicate twice, and the data are shown as mean \pm SD values. One of the representative pictures is shown.

edema formation by 54.5% ($P < 0.05$). Pretreatment in the priming phase (group 4: IR, 72.1%; $P < 0.01$) was found to be more effective for edema suppression than in the activation phase (group 5: IR, 29.5%; $P < 0.001$) and was comparable or higher in double pretreatment. In accordance with the TPA-induced enhancement of edema formation, an increase in epidermal thickness was observed with double TPA applications (Table 1 and Fig. 3, A and B; $12.2 \pm 1.6 \mu\text{m}$ in group 1 versus $29.1 \pm 3.3 \mu\text{m}$ in group 2; $P < 0.001$). Pretreatment with nobiletin in the priming stage (Table 1 and Fig. 3D; IR, 42.0%; $P < 0.001$ in group 4) was also more suppressive than that in the activation stage (Table 1 and Fig. 3E; IR, 59.2%; $P < 0.001$ in group 5). Double nobiletin pretreatment showed the highest inhibition (Table 1 and Fig. 3C; IR, 81.7%; $P < 0.001$ in group 3).

As shown in Table 1 and Fig. 3, A and B, a greater number of leukocytes were found to have infiltrated the dermis by double TPA application as compared with the control ($26.2 \pm 8.7/\text{mm}^2$ in group 1 versus $396.3 \pm 9.9/\text{mm}^2$ in group 2; $P < 0.001$; 15-fold). Double pretreatment with nobiletin-inhibited leukocyte infiltration by 76.9% ($P < 0.001$; Table 1 and Fig. 3C) and a single pretreatment in either the priming or activation phase also suppressed infiltration by 58.0 and 47.2%, respectively (Table 1 and Fig. 3, D and E).

Notably, the double TPA application dramatically increased the level of H_2O_2 in the mouse epidermis and dermis 7.5-fold (Table 1; $0.73 \pm 0.15 \text{ nmol/punch}$ in group 1 versus $5.47 \pm 0.28 \text{ nmol/punch}$ in group 2; $P < 0.001$). A higher inhibition by nobiletin was again observed when applied in the priming stage (IR, 57.2% in group 4; $P < 0.001$) than in the activation phase (IR 44.5% in group 4; $P < 0.001$). Double pretreatment with nobiletin showed the highest

Table 1 Inhibitory effects of nobiletin (NOB) on TPA-induced biological and histological parameters in mouse skin

Five ICR mice were used in one experimental group. Nobiletin [810 nmol in 100 μ l of acetone (Ac)] was topically applied to the shaved area of dorsal skin 30 min before application of a TPA solution (8.1 nmol/100 μ l of acetone). After 24 h, the same doses of nobiletin or acetone were applied 30 min prior to a second TPA application. Methods for measurement of biological activities are shown in "Materials and Methods." Statistical analysis was done by Student's *t* test.

Group	Edema (mg/punch)	Epidermal thickness (μ m)	Infiltrated leukocytes (No./mm ²)	H ₂ O ₂ (nmol/punch)	PCNA-labeling index (%)
1 (Ac/Ac→Ac/Ac)	24.7 ± 4.5	12.2 ± 1.6	26.2 ± 8.7	0.73 ± 0.15	15.7 ± 2.4
2 (Ac/TPA→Ac/TPA)	42.3 ± 2.6 ^a	29.1 ± 3.3 ^a	396.3 ± 9.9 ^a	5.47 ± 0.28 ^a	52.0 ± 4.1 ^a
3 (NOB/TPA→NOB/TPA)	32.7 ± 6.4 ^b	15.3 ± 1.0 ^c	111.7 ± 6.2 ^c	2.22 ± 0.39 ^c	24.0 ± 1.4 ^c
4 (NOB/TPA→Ac/TPA)	29.6 ± 4.9 ^d	19.1 ± 2.8 ^c	181.7 ± 73.1 ^c	2.78 ± 0.49 ^c	25.3 ± 2.9 ^c
5 (Ac/TPA→NOB/TPA)	37.1 ± 2.1 ^c	22.0 ± 2.2 ^c	221.7 ± 39.2 ^c	3.38 ± 0.35 ^c	31.3 ± 10.4 ^e

^a *P* < 0.001 (versus group 1).

^b *P* < 0.05 (versus group 2).

^c *P* < 0.001 (versus group 2).

^d *P* < 0.01 (versus group 2).

^e *P* < 0.02 (versus group 2).

inhibition of H₂O₂ production among the three inhibitory groups (IR, 69.1% in group 3; *P* < 0.001).

The PCNA-labeling index, a marker for cell proliferation, in the epidermis of the group 2 mice increased by 3.3-fold over that of group 1 (Table 1 and Fig. 4, A and B; 15.7 ± 2.4% in group 1 versus 52.0 ± 4.1% in group 2; *P* < 0.001). Pretreatment with either a single or double nobiletin application significantly reduced the PCNA-labeling indices (IRs, 57.0–73.6%; Table 1 and Fig. 4, C–E).

Inhibition of O₂⁻ Generation from Differentiated HL-60 Cells. We then examined the inhibitory effects of nobiletin in differentiated HL-60 cells, which are known to generate O₂⁻ with TPA stimulation. The inhibitory effect of a polyhydroxyflavonoid, luteolin, was compared with that of nobiletin, because resveratrol was unable to suppress O₂⁻ generation up to a concentration of 100 μ M (data not shown). As shown in Fig. 5A, TPA stimulation of differentiated HL-60 cells for 30 min led to marked extracellular O₂⁻ generation (27.9 ± 3.4 μ M in the media). Nobiletin demonstrated a much higher level of inhibition than did luteolin toward O₂⁻ generation accompanied by a complete suppression at concentrations of 20 and 100 μ M.

The IC₅₀ value of nobiletin (IC₅₀, 1.2 μ M) was approximately eight times lower than that of luteolin (IC₅₀, 9.8 μ M). No cytotoxicity was detected in any experiments (data not shown). As shown in Fig. 5B, the intracellular and extracellular ratios of nobiletin and luteolin, at a 100 μ M concentration 45 min after incubation, were found to be 0.108 ± 0.032 and 0.048 ± 0.010 (intracellular:extracellular), respectively. The intracellular luteolin was not detected at a concentration of 20 μ M.

Suppression of PGE₂ Production and COX-2 Protein Expression. Stimulation of RAW cells with LPS and IFN- γ for 18 h led to PGE₂ production in the media (15.1 ng/ml/mg protein; Fig. 6). Nobiletin suppressed PGE₂ production at the concentrations of 50 and 100 μ M (IRs, 35.8 and 41.2%, respectively), whereas resveratrol exhibited higher suppressive rates at the 25–100 μ M concentrations (IRs, 48.6%–100%). Stimulation of RAW 264.7 cells also led to a dramatic up-regulation of COX-2 protein expression by 90.9-fold (Fig. 6), which was hardly detectable in the control. Whereas nobiletin showed a dose-dependent suppression at a concentration range of 25–100 μ M (IRs, 50.7–90.4%), resveratrol showed marked inhibition only at a

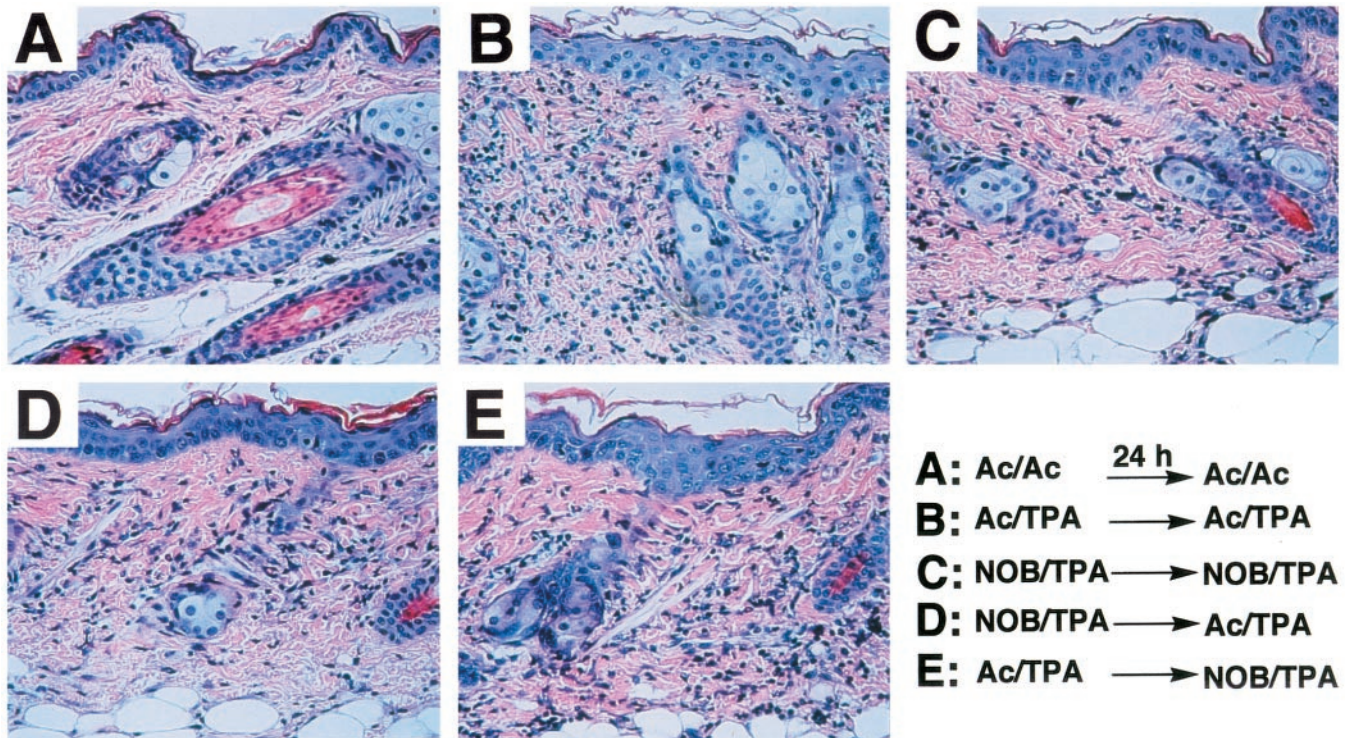


Fig. 3. Suppression by nobiletin of TPA-induced skin morphological changes observed by H&E staining. Three ICR mice were used in one experimental group. Nobiletin (810 nmol/100 μ l of acetone) was topically applied to the shaved area of dorsal skin 30 min before application of a TPA solution (8.1 nmol/100 μ l of acetone). After 24 h, the same doses of nobiletin or acetone were applied 30 min prior to a second TPA application. Methods for histological staining are described in "Materials and Methods." Ac, acetone; NOB, nobiletin.

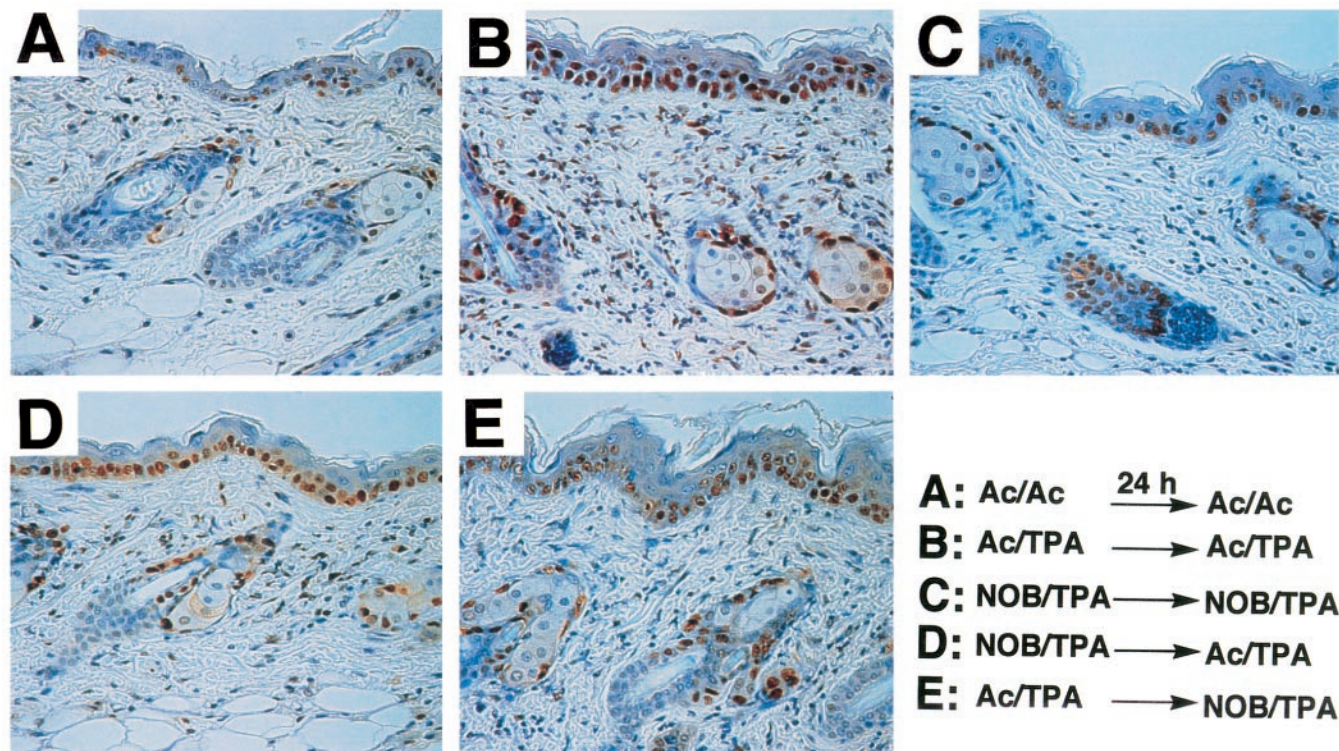


Fig. 4. Suppression by nobiletin of the TPA-induced increase in PCNA-positive cells in mouse epidermis. Three mice were used in one experimental group. Nobiletin (810 nmol/100 μ l of acetone) was topically applied to the shaved area of dorsal skin 30 min before application of a TPA solution (8.1 nmol/100 μ l of acetone). After 24 h, the same dosages of nobiletin or acetone were applied 30 min prior to a second TPA application. Methods for PCNA staining are described in "Materials and Methods." Ac, acetone; NOB, nobiletin.

concentration of 100 μ M, and its activity declined at a concentration range of 50 and 25 μ M. Notable cytotoxicity was not observed in any of the experiments (data not shown).

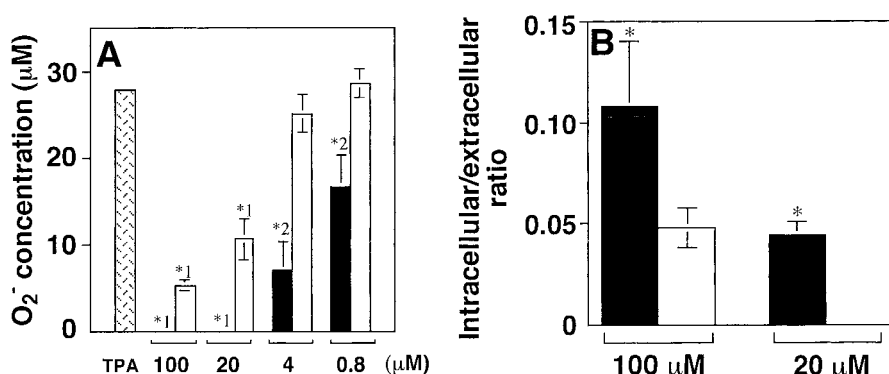
Antitumor-promoting Activity in Mouse Skin. We then examined the inhibitory effects of a topical application of nobiletin, at a dose range of 40–320 nmol, on tumor formation in DMBA (0.19 μ mol)-initiated and TPA (1.6 nmol)-promoted mouse skin. As shown in Table 2, the tumor incidence in the control group was 47.1% 20 weeks after promotion. In the four nobiletin-pretreated groups, the incidence was reduced by 33.5–43.3% (statistically not significant). The average number of tumors per mouse in the control was 2.06 ± 1.00 , and pretreatment with nobiletin at 160 and 320 nmol dose-dependently reduced them by 61.2% ($P < 0.01$) and 75.7% ($P < 0.01$), respectively.

DISCUSSION

Polymethoxyflavonoids including nobiletin occur exclusively in citrus fruit, and the Dancy tangerine has the highest total, containing

approximately 5 times the amount found in the peel of sweet orange varieties (e.g., *Citrus sinensis*; Ref. 35). Nobiletin and tangeretin, lacking a single methoxyl group that is present in nobiletin, occur at the concentrations of 46 and 7 ppm, respectively, in Valencia orange juice (40). Nobiletin has previously been reported to induce differentiation of mouse myeloid leukemia cells (41), to exhibit antiproliferative activity toward a human squamous cell carcinoma cell line (42), to exert antimutagenic activity (43), and to suppress the induction of matrix metalloproteinase-9 (44). In addition, tangeretin was reported to inhibit tumor invasion and metastasis (45) and to induce apoptosis in HL-60 cells (46). The present study shows that nobiletin suppresses both LPS and IFN- γ -induced NO_2^- production in a dose-dependent manner (Fig. 2). Whereas resveratrol was reported to suppress iNOS expression through down-regulation of nuclear factor- κ B activity (37), the action mechanism of nobiletin for iNOS suppression is unclear. In addition, issues of whether nobiletin directly inhibits iNOS activity and affects both neural and endothelial NOS functions remain to be addressed.

Fig. 5. Inhibitory effects of nobiletin and luteolin on TPA-induced O_2^- generation in differentiated HL-60 cells and their cellular uptake. In A, differentiated HL-60 cells (1×10^6 cells/ml) were stimulated by 100 nM TPA to induce O_2^- , the extracellular concentration of which was measured by the cytochrome *c* method. Test compounds were added at concentrations of 0.8, 4, 20, and 100 μ M. \square , nobiletin. \square , luteolin. *1, $P < 0.001$; *2, $P < 0.01$ versus the group treated only with TPA in Student's *t* test. In B, nobiletin (\blacksquare) or luteolin (\square , 100 or 20 μ M each) was added to 1 ml of differentiated HL-60 cell suspension (1×10^6 cells/ml), and the mixture thus obtained was incubated at 37°C for 45 min. Intracellular and extracellular contents of the test compounds were determined using HPLC. *, $P < 0.001$ versus the group treated with luteolin in Student's *t* test. Each experiment was done independently in duplicate twice, and the data are shown as mean \pm SD values.



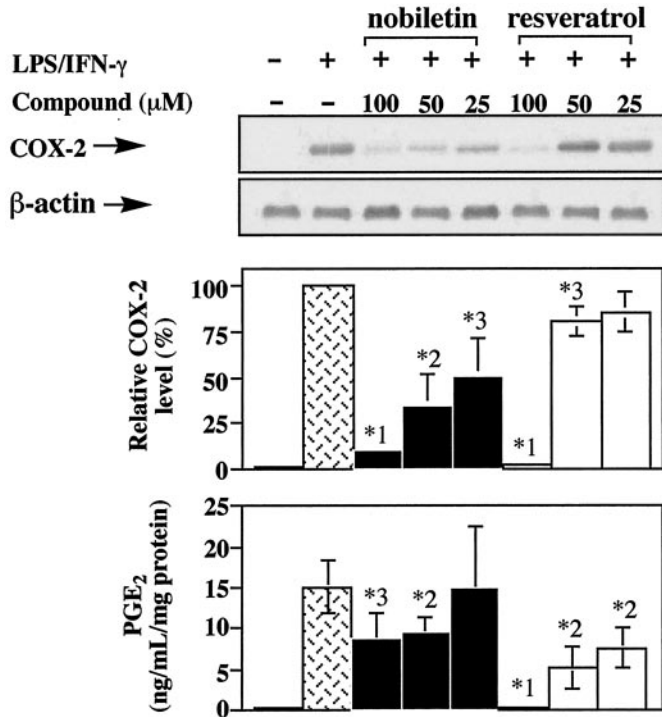


Fig. 6. Suppression by nobiletin and resveratrol of LPS/IFN- γ -induced PGE₂ production and COX-2 protein expression in RAW 264.7 cells. RAW 264.7 cells were incubated with LPS (100 ng/ml), IFN- γ (100 units/ml), and DMSO [0.5% (v/v) as a final concentration], or with test compounds (25, 50, or 100 μ M) for 18 h. The PGE₂ concentrations were determined using a commercial experimental kit (Cayman, Ann Arbor, MI). Western blotting was performed as described in "Materials and Methods." The COX-2 band levels were corrected by those of β -actin as the internal standard. *1, $P < 0.001$; *2, $P < 0.01$; *3, $P < 0.02$ versus positive control (LPS/IFN- γ) in the Student t test. One of the representative pictures is shown. Each experiment was done independently in duplicate twice, and the data are shown as mean \pm SD values.

As summarized in Table 1, nobiletin inhibited double-TPA-application-induced biological and histological parameters relating to oxidative damage and inflammation. Nobiletin notably suppressed all of the parameters in both the priming and the activation stages. The inhibitory effects of the double nobiletin pretreatment appear to be caused by the additive effects of each application in both stages because the double pretreatments were most suppressive.

TPA has recently been reported to produce NO and VEGF in human polymorphonuclear leukocytes (24, 46–48). Overexpressed VEGF leads to the induction of vascular hyperpermeability (25). On the other hand, PGE₂ is well known to increase vascular permeability. Nobiletin inhibited the expression of COX-2 protein, which is an inducible and rate-limiting enzyme for PG synthesis (Fig. 6). Accordingly, nobiletin inhibited the release of PGE₂ from RAW 264.7 cells (Fig. 6) and also from rabbit synovial cells (44). Although we have not examined the effects of nobiletin on vascular permeability, the inhibition by nobiletin of edema formation and the reduction of epidermal thickness (Table 1 and Fig. 3, C–E) may be partly attributable to the suppression of NO, VEGF, and PGE₂ production.

As shown in Table 1 and Fig. 3, leukocyte infiltration, a critical step in the priming stage, was successfully suppressed by nobiletin in both stages. After TPA application to mouse skin, an increased release of IL-1 (a cytokine involved in immune and inflammatory events) becomes predominant (49). There are two distinct forms of IL-1, namely, IL-1 α and IL-1 β . Of these cytokines, IL-1 α is especially noted as an important chemotactic factor released from keratinocytes in the skin carcinogenesis model because its release involves cell proliferation and hyperplasia in the tumor-promoting stage *via* autocrine regulation (49). On the other hand, LPS-stimulated RAW 264.7

cells release TNF- α , IL-1 β , and IL-6 (50), and, recently, we found that nobiletin inhibited the release of both LPS-induced and IFN- γ -induced TNF- α and IL-1 β from RAW 264.7 cells (data not shown). Additional studies on the influence of nobiletin on cytokine regulations may elucidate the action mechanism(s) by which nobiletin suppresses leukocyte infiltration.

Because nobiletin did not significantly scavenge O₂⁻ generated from the xanthine/xanthine oxidase system nor inhibit xanthine oxidase activity up to a concentration of 500 μ M (data not shown), it may inhibit the assembly or activity of a multicomponent NADPH oxidase system in differentiated HL-60 cells (Fig. 5A). This inhibitory mode, *i.e.*, not radical scavenging but generation inhibition, is also found in NO generation. A chemical characteristic of nobiletin, which bears none of the hydroxyl groups that are indispensable for O₂⁻ scavenging activity, explains such an inhibitory mode. Possessing no hydroxyl groups may occasionally give some advantages to nobiletin in terms of antioxidation because, although being reported to exhibit antioxidative activities in rat liver microsomes, some polyhydroxyflavonoids change to become pro-oxidants to generate H₂O₂ (51).

Nobiletin possesses a much higher ability to inhibit O₂⁻ generation than does luteolin (Fig. 5A). A predominance of polymethoxyflavonoids over polyhydroxyflavonoids was also observed in antitumor activities using a cell culture system (42). Differences in their activities may be derived from the relatively greater membrane uptake efficiencies of polymethoxyflavonoids than those of polyhydroxyflavonoids because methoxylation of the phenolic hydroxyl groups, in general, increases the molecular hydrophobicity that regulate incorporation rates. In fact, intracellular content of nobiletin was approximately two times higher than that of luteolin in differentiated HL-60 cells when incubated at a concentration of 100 μ M (Fig. 5B).

Double-TPA-application-induced H₂O₂ production *in vivo* was markedly inhibited by the pretreatment(s) of nobiletin (Table 1). Decreased levels of H₂O₂ may be attributable to the inhibition of O₂⁻ generation because H₂O₂ is mostly derived from O₂⁻ as a function of O₂⁻ dismutase or nonenzymatically. Nobiletin, a dual inhibitor of both O₂⁻ and NO radical generation, can be recognized as a potent, naturally occurring anti-inflammatory agent, because peroxyxynitrite, a coupling product of O₂⁻ and NO, enhances COX-2 activity (52), involving inflammatory processes and thereby leading to carcinogenesis. By contrast, resveratrol was a selective inhibitor of NO generation (Fig. 2).

Certain ROS, such as H₂O₂, and proinflammatory cytokines including TNF- α are reported to cause cell death, which is occasionally attributable to apoptosis (53). Conversely, cell injury and cell death are manifest in TPA-applied mouse skin. Compensatory growth is subsequently necessary and is induced by growth factors such as transforming growth factor α and β and keratinocyte growth factor, all of which are inducible by TPA (54–56). Double TPA applications promoted cell growth, as revealed by increased PCNA-labeling indices, and resulted in epidermal hyperplasia and edema formation (Table 1, and Fig. 4, A and B). Pretreatment with nobiletin decreased cell growth rates (Table 1, and Fig. 4, C–E), possibly because of the escaping of epidermal cells from oxidative cellular death, which diminished the growth factor production in surrounding cells.

Table 2. Antitumor-promoting activity of nobiletin in DMBA-initiated ICR mouse skin

Group	No. of mice	Incidence, % (% inhibition)	No. of tumors/mouse (% inhibition)
DMBA + TPA	17	47.1	2.06 \pm 1.00
+ nobiletin (40 nmol)	16	31.1 (33.5)	1.63 \pm 0.87 (20.9)
+ nobiletin (80 nmol)	16	31.1 (33.5)	1.94 \pm 0.98 (5.8)
+ nobiletin (160 nmol)	15	26.7 (43.3)	0.80 \pm 0.48 (61.2) ^a
+ nobiletin (320 nmol)	16	31.1 (33.5)	0.50 \pm 0.22 (75.7) ^a

^a $P < 0.001$ in Welch's t test.

As predicted by the suppressive efficacies of biochemical markers relating to oxidative stress and inflammation (Figs. 2–6), topical application of nobiletin at doses of 160 and 320 nmol inhibited the multiplicity of skin tumors in a dose-dependent manner (Table 2). The chemopreventive efficacy of nobiletin in the mouse skin model may be superior to that of resveratrol, which inhibited tumor formation at the dose range of 1–25 μ mol although experimental conditions were different (39). In any case, this is the first report demonstrating the chemopreventive ability of nobiletin in an animal model.

In conclusion, our approach, *i.e.*, searching for iNOS induction inhibitors by activity-guiding separation, may be a promising strategy for discovering effective chemopreventive agents. Citrus flavonoid nobiletin was found to be a functionally novel antitumor promoter by working in both the priming and activation stages in mouse skin. It is also notable that it exclusively occurs in citrus fruits, is chemically stable, and is suitable for mass preparation for a variety of rodent studies. Nobiletin is currently being investigated by our collaborative research group for its chemopreventive efficacies in other inflammation-associated carcinogenesis models.

ACKNOWLEDGMENTS

We thank H. Sakai, S. Iwamoto, and K. Kawabata for their technical assistance.

REFERENCES

- Steinmetz, K. A., and Potter, J. D. Vegetables, fruits, and cancer. I. Epidemiology. *Cancer Causes Control*, 2: 325–357, 1991.
- Lam, L. K. T., Zhang, J., Hasegawa, S., and Schut, H. A. J. Inhibition of chemically induced carcinogenesis by citrus limonoids. In: M-T. Huang, T. Osawa, C-T. Ho, and R. T. Rosen (eds.), *Food Phytochemicals for Cancer Prevention I*, ASC Symposium Series 546, pp. 209–219. Washington, D. C.: American Chemical Society, 1994.
- Miller, E. G., Gonzales-Sanders, A. P., Couvillon, A. M., Wight, J. M., Hasegawa, S., Lam, L. K. T., and Sunahara, G. I. Inhibition of oral carcinogenesis by green coffee beans and limonoid glucosides. In: M-T. Huang, T. Osawa, C-T. Ho, and R. T. Rosen (eds.), *Food Phytochemicals for Cancer Prevention I*, ASC Symposium Series 546, pp. 220–229. Washington, D. C.: American Chemical Society, 1994.
- Kawamori, T., Tanaka, T., Hirose, M., Ohnishi, M., and Mori, H. Inhibitory effects of *d*-limonene on the development of colonic aberrant crypt foci induced by azoxymethane in F344 rats. *Carcinogenesis (Lond.)*, 17: 369–372, 1996.
- Crowell, P. L., Kennan, W. S., Haag, J. D., Ahmad, S., Vedejs, E., and Gould, M. N. Chemoprevention of mammary carcinogenesis by hydroxylated derivatives of *d*-limonene. *Carcinogenesis (Lond.)*, 13: 1261–1264, 1992.
- Le Bon, A. M., Ziegler, L., and Suschetet, M. Comparison of hydroxylated and non-hydroxylated natural flavonoids as *in vitro* modulations of rat hepatic benzo(*a*)pyrene metabolism. In: I. T. Waldron, I. T. Johnson, and G. R. Fenwick (eds.), *Food and Cancer Prevention: Chemical and Biological Aspects*, pp.217–222. Cambridge: The Royal Society of Chemistry, 1993.
- Tanaka, T., Makita, H., Ohnishi, M., Hirose, Y., Wang, A., Mori, H., Satoh, K., Hara, A., and Ogawa, H. Chemoprevention of 4-nitroquinoline 1-oxide-induced oral carcinogenesis by dietary curcumin and hesperidin: comparison with the protective effect of β -carotene. *Cancer Res.*, 54: 4653–4659, 1994.
- Tanaka, T., and Mori, H. Inhibition of colon carcinogenesis by non-nutritive constituents in foods. *J. Toxicol. Pathol.*, 9: 139–149, 1996.
- Murakami, A., Nakamura, Y., Koshimizu, K., and Ohigashi, H. Glyceroglycolipids from *Citrus hystrix*, a traditional herb in Thailand, potently inhibits the tumor promoting activity of 12-*O*-tetradecanoylphorbol-13-acetate in mouse skin. *J. Agric. Food Chem.*, 43: 2779–2783, 1995.
- Murakami, A., Kuki, W., Takahashi, Y., Yonei, H., Nakamura, Y., Ohto, Y., Ohigashi, H., and Koshimizu, K. Auraptene, a citrus coumarin, inhibits 12-*O*-tetradecanoylphorbol-13-acetate-induced tumor promotion in ICR mouse skin, possibly through suppression of superoxide generation in leukocytes. *Jpn. J. Cancer Res.*, 88: 443–452, 1997.
- Tanaka, T., Kawabata, K., Kakumoto, M., Matsunaga, K., Mori, H., Murakami, A., Kuki, W., Takahashi, Y., Yonei, H., Sastoh, K., Hara, A., Maeda, M., Ota, T., Odashima, S., Koshimizu, K., and Ohigashi, H. Chemoprevention of 4-nitroquinoline 1-oxide-induced oral carcinogenesis by citrus auraptene in rats. *Carcinogenesis (Lond.)*, 19: 425–431, 1998.
- Tanaka, T., Kawabata, K., Kakumoto, M., Makita, H., Hara, A., Mori, H., Satoh, K., Murakami, A., Kuki, W., Takahashi, Y., Yonei, H., Koshimizu, K., and Ohigashi, H. Citrus auraptene inhibits chemically induced colonic aberrant crypt foci in F344 rats. *Carcinogenesis (Lond.)*, 18: 2155–2161, 1997.
- Tanaka, T., Kawabata, K., Kakumoto, M., Hara, A., Murakami, A., Kuki, W., Takahashi, Y., Yonei, H., Maeda, M., Ota, T., Odashima, S., Yanane, T., Koshimizu, K., and Ohigashi, H. Citrus auraptene exerts dose-dependent chemopreventive activity in rat large bowel tumorigenesis: the inhibition correlates with suppression of cell proliferation and lipid peroxidation and with induction of Phase II drug-metabolizing enzymes. *Cancer Res.*, 58: 2550–2556, 1998.
- Vanvaskas, S., and Schmidt, H. H. H. W. Just say NO to cancer? *J. Natl. Cancer Inst.*, 89: 406–407, 1997.
- Nathan, C., and Xie, Q. Nitric oxide synthases: roles, tolls, and controls. *Cell*, 78: 915–918, 1994.
- Ohshima, H., and Bartsch, H. Chronic infections and inflammatory processes as cancer risk factors: possible role of nitric oxide in carcinogenesis. *Mutat. Res.*, 305: 253–264, 1994.
- Xie, K., Huang, S., Dong, Z., Juang, S. H., Wang, Y., and Fidler, I. J. Destruction of bystander cells by tumor cells transfected with inducible nitric oxide (NO) synthase gene. *J. Natl. Cancer Inst.*, 89: 421–427, 1997.
- Tsuji, S., Kawano, S., Tsuji, M., Takei, Y., Tanaka, M., Sawaoka, H., Nagano, K., Fusamoto, H., and Kamada, T. *Helicobacter pylori* extract stimulates inflammatory nitric oxide production. *Cancer Lett.*, 108: 195–200, 1996.
- Arroyo, P. L., Hatch-Pigott, V., Mower, H. F., and Cooney, R. V. Mutagenicity of nitric oxide and its inhibition by antioxidants. *Mutat Res.*, 281: 193–202, 1992.
- Wink, D. A., Kasprzak, K. S., Maragos, C. M., Elespuru, R. K., Misra, M., Dunams, T. M., Cebula, T. A., Koch, W. H., Andrews, A. W., Allen, J. S., and Keefer, L. K. DNA deaminating ability and genotoxicity of nitric oxide and its progenitors. *Science (Washington DC)*, 254: 1001–1003, 1991.
- Miwa, M., Stuehr, D. J., Marletta, M. A., Wishnok, J. S., and Tannenbaum, S. R. Nitrosation of amines by stimulated macrophages. *Carcinogenesis (Lond.)*, 8: 955–958, 1987.
- Teixeira, M. M., Williams, T. J., and Hellewell, P. G. Role of prostaglandin and nitric oxide in acute inflammatory reactions in guinea-pig skin. *Br. J. Pharmacol.*, 110: 1515–1521, 1993.
- Ahmad, N., Srivastava, R. C., Agarwal, R., and Mukhtar, H. Nitric oxide synthase and skin tumor promotion. *Biochem. Biophys. Res. Commun.*, 232: 328–331, 1997.
- Xiong, M., Elson, G., Legarda, D., and Leibovich, S. J. Production of vascular endothelial growth factor by murine macrophages: regulation by hypoxia, lactate, and the inducible nitric oxide synthase pathway. *Am. J. Pathol.*, 153: 587–598, 1998.
- Larcher, F., Murillas, R., Bolontrade, M., Conti, C. J., and Jorcano, J. L. VEGF/VPF overexpression in skin of transgenic mice induces angiogenesis, vascular hyperpermeability and accelerated tumor development. *Oncogene*, 17: 303–311, 1998.
- Mueller, D. K., Kopp, S. A., Marks, F., Seibert, K., and Fuerstenberger, G. Localization of prostaglandin H synthase isoenzymes in murine epidermal tumors: suppression of skin tumor promotion by inhibition of prostaglandin H synthase-2. *Mol. Carcinog.*, 23: 36–44, 1998.
- Puigero, V., and Queralt, J. Effect of topically applied cyclooxygenase-2-selective inhibitors on arachidonic acid- and tetradecanoylphorbol acetate-induced dermal inflammation in the mouse. *Inflammation*, 21: 431–442, 1997.
- Ohata, T., M. Fukuda, Takahashi, M., Sugimura, T., and Wakabayashi, K. Suppression of nitric oxide production in lipopolysaccharide-stimulated macrophage cells by ω 3 polyunsaturated fatty acids. *Jpn. J. Cancer Res.*, 88: 234–237, 1997.
- Ohata, T., Fukuda, K., Murakami, A., Ohigashi, H., Sugimura, T., and Wakabayashi, K. Inhibition by 1'-acetoxychavicol acetate of lipopolysaccharide- and interferon- γ -induced nitric oxide production through suppression of inducible nitric oxide synthase gene expression in RAW264 cells. *Carcinogenesis (Lond.)*, 19: 1007–1012, 1998.
- Chan, M. M.-Y., Ho, C.-T., and Huang, H.-I. Effects of three dietary phytochemicals from tea, rosemary, and turmeric on inflammation-induced nitrite formation. *Cancer Lett.*, 96: 23–29, 1995.
- Soliman, K. F. A., and Mazzi, E. A. *In vitro* attenuation of nitric oxide production in C6 astrocyte cell culture by various dietary compounds. *Proc. Soc. Exp. Biol. Med.*, 218: 390–397, 1998.
- Kim, O. K., Murakami, A., Nakamura, Y., and Ohigashi, H. Screening of edible Japanese plants for nitric oxide generation inhibitory activities in RAW 264.7 cells. *Cancer Lett.*, 125: 199–207, 1998.
- Wei, H. Wei, L., Frenkel, K. Bowen, R., and Barnes, S. Inhibition of tumor promoter-induced hydrogen peroxide formation *in vitro* and *in vivo* by genistein. *Nutr. Cancer*, 20: 1–12, 1993.
- Ji, C., and Marnett, L. J. Oxygen radical-dependent epoxidation of (7S,8S)-dihydroxy-7,8-dihydrobenzo[*a*]pyrene in mouse skin *in vivo*. Stimulation by phorbol esters and inhibition by anti-inflammatory steroids. *J. Biol. Chem.*, 267: 17842–17878, 1992.
- Chen, J., Montanari, A. M., and Widmer, W. W., Two new polymethoxylated flavonoids, a class of compounds with potential anticancer activity, isolated from cold pressed Dancy tangerine peel oil solids. *J. Agric. Food Chem.*, 45: 364–368, 1997.
- Nakamura, Y., Murakami, A., Ohto, Y., Torikai, K., Tanaka, T., and Ohigashi, H. Suppression of tumor promoter-induced oxidative stress and inflammatory responses in mouse skin by a superoxide generation inhibitor 1'-acetoxychavicol acetate. *Cancer Res.*, 58: 4832–4839, 1998.
- Tsai, S. H., Kin-Shiau, S. Y., and Lin, J. K. Suppression of nitric oxide synthase and the down-regulation of the activation of NF- κ B in macrophages by resveratrol. *Br. J. Pharmacol.*, 126: 673–680, 1999.
- Subbaramaiah, K., Chung, W. J., Michaluart, P., Telang, N., Tanabe, T., Inoue, H., Jang, M., Pezzuto, J. M., and Dannenberg, A. J. Resveratrol inhibits cyclooxygenase-2 transcription and activity in phorbol ester-treated human mammary epithelial cells. *J. Biol. Chem.*, 273: 21875–21882, 1998.
- Jang, M., Cai, L., Udeani, G. O., Slowing, K. V., Thomas, C. F., Beecher, C. W., Fong, H. H., Farnsworth, N. R., Kinghorn, A. D., Mehta, R. G., Moon, R. C., and Pezzuto, J. M. Cancer chemopreventive activity of resveratrol, a natural product derived from grapes. *Science (Washington DC)*, 275: 218–220, 1997.
- Kawai, S., Tomono, Y., Katase, E., Ogawa, K., and Yano, M. HL-60 differentiating activity and flavonoid content of the readily extractable fraction prepared from *Citrus* juices. *J. Agric. Food Chem.*, 47: 128–135, 1999.

41. Sugiyama, S., Umemura, K., Kuroyanagi, M., Ueno, A., and Taki, T. Studies on the differentiation inducers of myeloid leukemic cells from *Citrus* species. *Chem. Pharm. Bull.*, *41*: 714–719, 1993.
42. Kandawaswami, C., Perkins, E., Soloniuk, D. S., Drzewiecki, and Middleton, E., Jr. Antiproliferative effects of citrus flavonoids on a human squamous cell carcinoma *in vitro*. *Cancer Lett.*, *56*: 147–152, 1991.
43. Wall, M. W., Wani, M. C., Manukumar, G., Abraham, P., Taylor, H., Hughes, T. J., Warner, J., and McGivney, R. Plant antimutagenic agents, 2. Flavonoids. *J. Nat. Prod. (Lloydia)*, *51*: 1084–1091, 1998.
44. Ishiwa, J., Sato, T., Mimaki, Y., Sashida, Y., Yano, M., and Ito, A. A citrus flavonoid, nobiletin, suppresses production and gene expression of matrix metalloproteinase 9/gelatinase B in rabbit synovial fibroblasts. *J. Rheumatol.*, *27*: 20–25, 2000.
45. Bracke, M. E., Bruyneel, E. A., Vermeulen, S. J., Vennekens, K., Marck, V. V., and Mareel, M. M. Citrus flavonoid effect on tumor invasion and metastasis. *Food Technol.*, *48*: 121–124, 1994.
46. Hirano, T., Abe, K., Gotoh, M., and Oka, K. Citrus flavone tangeretin inhibits leukaemic HL-60 cell growth partially through induction of apoptosis with less cytotoxicity on normal lymphocytes. *Br. J. Cancer*, *72*: 1380–1388, 1995.
47. Gaudry, M., Bregerie, O., Andrieu, V., El-Benna, J., Pocardalo, M. A., and Hakim, J. Intracellular pool of vascular endothelial growth factor in human neutrophils. *Blood*, *90*: 4153–4161, 1997.
48. Stolarek, R., Kula, P., Kurmanowska, Z., and Nowak, D. Effect of various agonists on nitric oxide generation by human polymorphonuclear leukocytes. *Int. J. Clin. Lab. Res.*, *28*: 104–109, 1998.
49. Fischer, S. M., Lee, W. Y. L., and Locniskar, M. F. The pro-inflammatory and hyperplasiogenic action of interleukin-1 α in mouse skin, pp. 161–177. *In*: R. M. McClain, T. J. Slaga, LeBoeuf, and H. Pitot (eds.), *Growth Factors and Tumor Promotion: Implications for Risk Assessment*. New York: Wiley-Liss, Inc., 1995.
50. Adams, J. L., and Czuprynski, C. J. Mycobacterial cell wall components induce the production of TNF- α , IL-1, and IL-6 by bovine monocytes and the murine macrophage cell line RAW 264.7. *Microb. Pathog.*, *16*: 401–411, 1994.
51. Miura, Y. H., Tomita, I., Watanabe, T., Hirayama, T., and Fukui, S. Active oxygens generation by flavonoids. *Biol. Pharm. Bull.*, *21*: 93–96, 1998.
52. Landino, L. M., Crews, B. C., Timmons, M. D., Morrow, J. D., and Marnett, L. J. Peroxynitrite, the coupling product of nitric oxide and superoxide, activates prostaglandin biosynthesis. *Proc. Natl. Acad. Sci. USA*, *93*: 15069–15074, 1996.
53. Riou, C., Remy, C., Rabilloud, R., Rousset, B., and Fonlupt, P. H₂O₂ induces apoptosis of pig thyrocytes in culture. *J. Endocrinol.*, *156*: 315–322, 1998.
54. Imamoto, A., Beltran, L., and DiGiovanni, J. Evidence for autocrine/paracrine growth stimulation by transforming growth factor- α during the process of skin tumor promotion. *Mol. Carcinog.*, *4*: 52–60, 1991.
55. Parkinson, K., and Balmain, A. Chalcones revisited: a possible role for transforming growth factor- β in tumor promotion. *Carcinogenesis (Lond.)*, *11*: 195–198, 1990.
56. Werner, S., Peters, K. G., Longaker, M. T., Fuller-Pace, F., Banda, M. J., and Williams, L. T. Large induction of keratinocytes growth factor expression in the dermis during wound healing. *Proc. Natl. Acad. Sci. USA*, *89*: 6896–6900, 1982.

Cancer Research

The Journal of Cancer Research (1916–1930) | The American Journal of Cancer (1931–1940)

Inhibitory Effect of Citrus Nobiletin on Phorbol Ester-induced Skin Inflammation, Oxidative Stress, and Tumor Promotion in Mice

Akira Murakami, Yoshimasa Nakamura, Koji Torikai, et al.

Cancer Res 2000;60:5059-5066.

Updated version Access the most recent version of this article at:
<http://cancerres.aacrjournals.org/content/60/18/5059>

Cited articles This article cites 49 articles, 11 of which you can access for free at:
<http://cancerres.aacrjournals.org/content/60/18/5059.full#ref-list-1>

Citing articles This article has been cited by 9 HighWire-hosted articles. Access the articles at:
<http://cancerres.aacrjournals.org/content/60/18/5059.full#related-urls>

E-mail alerts [Sign up to receive free email-alerts](#) related to this article or journal.

Reprints and Subscriptions To order reprints of this article or to subscribe to the journal, contact the AACR Publications Department at pubs@aacr.org.

Permissions To request permission to re-use all or part of this article, use this link
<http://cancerres.aacrjournals.org/content/60/18/5059>.
Click on "Request Permissions" which will take you to the Copyright Clearance Center's (CCC) Rightslink site.